wavelength of 0.65 μm for Al_2O_3 in the process of heating for the first (a) and second (b) sphere passages over the specimen. In the second oscillogram one can clearly see the peak produced by the flash. Figure 3 shows results of measurements of the directional spectral radiation coefficients for Al_2O_3 in the brightness temperature range 2080-2375 K.

The uncertainty in the measurements of the hemispherically directional spectral reflection coefficient does not exceed 2%, while the uncertainty in measurements of the thermodynamic temperature of the irradiated surface over the range 2000-2500 K comprised 0.5%.

NOTATION

$E^0_{\lambda T}$, spectral radiation density of black body at temperature T; $E^0_{\lambda Tb}$, spectral radiation density of black body at temperature T_b; C_1, constant in Planck radiation law, $C_1 = 3.7413 \cdot 10^{-16}$ W/m^2; C_2, constant in Planck radiation law, $c_2 = 1.4388 \cdot 10^4$ μ·deg; λ, wavelength, μm; T, temperature, deg; T_b, brightness temperature, deg; θ, polar angle; φ, azimuthal angle; dω, elementary solid angle; $\varepsilon_\lambda(\theta, \varphi, T)$ directional spectral emissivity; $\alpha_\lambda(\theta, \varphi, T)$ directional spectral absorption capability; $\rho_\lambda(2\pi, \theta, \varphi, T)$ directional hemispherical spectral reflection coefficient: $\rho_{B\lambda}(2\pi, \theta, \varphi)$, hemispherical directional spectral reflection coefficient of MS-20 milk glass; $L(2\pi, \theta, \varphi)$, specimen brightness in direction defined by angles θ from entire hemisphere; L_0; sphere wall brightness.

LITERATURE CITED

1. M. Bober, H. U. Korow, and K. Muller, High Temperatures – High Pressures, Vol. 12 (1980), pp. 161-168.
2. M. Bober, High Temperatures – High Pressures, Vol. 12 (1980), pp. 297-306.
3. A. Yu. Basharin, A. V. Kirillin, and M. A. Sheidlin, Teplofiz. Vys. Temp., 22, No. 1, 131-137 (1984).
4. A. Yu. Basharin, A. V. Kirillin, M. A. Sheindlin, and L. M. Kheifets, Teplofiz. Vys. Temp., 24, No. 1, 76-81 (1984).
5. V. N. Snopko, Spectral Methods for Optical Pyrometry of a Heated Surface [in Russian], Minsk (1988).
6. R. Zigel' and Howell, Heat Exchange by Radiation [in Russian], Moscow (1975).

RADIATIVE PROPERTIES OF COMPOSITE MATERIALS BASED ON PHENOLIC CARBON AND GLASS REINFORCED PLASTICS

M. Ya. Flyaks

UDC 535.231:535.243.2

The article investigates the change of radiative characteristics of composites based on carbon, quartz, and glass fabric and phenol formaldehyde resin in dependence on the wavelength, the temperature, and thermal effects.

Information on the radiative properties of composite materials (CM) is indispensable for the solution of problems of heat exchange, and also for the calculation and design of structures subjected to intense thermal loading. Investigation of the behavior of the radiative characteristics of CM in dependence on the temperature and other factors is also required when new compositions are devised, for their comparative evaluation and the selection of the most promising ones.

Materials based on composites of heat-resistant fabrics and phenol formaldehyde resin are in practice one of the most important groups of heat-protective coatings. They can be used for the protection of surfaces in a broad range of thermal fluxes including very large

A. V. Lykov Institute of Heat and Mass Exchange, Academy of Sciences of the Belorussian SSR, Minsk.

Translated from Inzhenerno-fizicheskii Zhurnal, Vol. 61, No. 4, pp. 663-668, October, 1991. Original article submitted November 21, 1990.

0022-0841/91/6104-1288$12.50

ones [1]. However, published data on the radiative properties of phenol plastics are very limited and of a fragmentary nature [2]. For instance, articles [3, 4] provide information on the spectral radiant emittance of coke residues of phenolic carbon (T = 2550, 2850 K) and phenolic nylon (T = 2770-3000 K) in the range 0.4-2.8 μm. Chang et al. [5] presented data on $\varepsilon_{\lambda n}$ of phenolic graphite at 2500 K for the range 0.3-10 μm, and Pope [6] presented the results of the determination of the integral degree of blackness of the cokes of phenolic nylon resins. Of the greatest interest are the radiative properties of phenol plastics with different fillers in the temperature range 1200-2000 K which is very important for practice. The point is that at these temperatures the radiative properties of coatings are not determined solely by the characteristics of the coke residues of phenol formaldehyde resin but also to a considerable extent by the properties of the fabrics; this may lead to a considerable difference in the spectral and temperature dependence of the thermoradiative characteristics of composites with different fillers.

The present article submits the results of investigations of the radiative properties of CM based on composites of carbon, quartz, and glass fabrics, and on phenol formaldehyde resin. Experimental data were obtained on the dependence of the normally hemispherical reflectivity $\rho_{\lambda n}$ on the wavelength 0.58 μm on the temperature in the range 1200-2000 K of the mentioned CM before and after treatment in plasma flux. We present the results of the determination of the spectral normal radiant emittance $\varepsilon_{\lambda n}$ in the range 1-10 μm at T = 1200-2000 K. From the measured values of $\varepsilon_{\lambda n}$ we calculated the values of the integral normal degree of blackness $\varepsilon_{\Sigma n}$. According to the evaluations the relative error of determining $\varepsilon_{\lambda n}$ in the range 1-10 μm and of the value of $\varepsilon_{\lambda n} = 1 - \rho_{\lambda n}$ on the wavelength 0.58 μm did not exceed 4% at a confidence level of at least 0.95. The measurements were carried out at a vacuum of 13-1.3 Pa (10^{-1}-10^{-2} mm Hg).

The data on the normally hemispherical reflectivity $\rho_{\lambda n}$ on the wavelength 0.58 μm can be used for calculating radiant emittance in accordance with Kirchhoff's law, with subsequent pyrometric determination of the temperature of heat-protective coatings. They can be used for evaluating the behavior of the optical characteristics in the visible range upon change of temperature. Since the radiant emittance of the structural components of CM, viz., coke residue of phenol formaldehyde resin—carbon, quartz, glass, in the visible range barely changes with wavelength, it is natural to assume that composites based on them are predominantly gray in the visible range.

The normally hemispherical reflectivity was determined by comparing radiation from the specimen and from a standard (magnesium oxide) by the formula

$$\rho_{\lambda n} = \left(\frac{I^{s}_{\lambda n}}{I^{st}_{\lambda n}} - \frac{I^{o}_{\lambda n}}{I^{st}_{\lambda n}}\right) \rho^{st}_{\lambda n}, \qquad (1)$$

where $I^{s}_{\lambda n}$, $I^{o}_{\lambda n}$, $I^{st}_{\lambda n}$ are, respectively, the spectral densities of the brightness of the summary radiation of the specimen, of the brightness of the proper radiation of the specimen, and of the brightness of the standard; $\rho^{st}_{\lambda n}$ is the reflectivity of the standard (for the value of $\rho^{st}_{\lambda n}$ was determined beforehand in an independent manner). For diffuse illumination of the specimen we used an integrating sphere and sources with a line spectrum, viz., high-pressure quartz mercury lamps. The specimen was heated by beams of continuous CO_2 lasers with working wavelength 10.6 μm. The proper radiation was separated from the reflected radiation by recording the brightness of the specimen $I^{s}_{\lambda n}$ due to proper and reflected radiation in the lines of radiation of mercury vapors (λ_i = 0.577; 0.579 μm) and the intensity of the proper radiation $I^{o}_{\lambda n}$ on the wavelength λ_j = 60 μm. Here it was assumed that in consequence of the closeness of λ_i and λ_j the equality $\varepsilon_{\lambda n}(\lambda_i) = \varepsilon_{\lambda n}(\lambda_i)$ is correct. A detailed description of the method and of the installation is presented in [7, 8].

Figure 1 presents the results of the determination of $\rho_{\lambda n}$ of the investigated CM. It can be seen from Fig. 1a, b that for phenol plastics with quartz and glass fabric as filler there exists a strong dependence of $\rho_{\lambda n}$ on the temperature. With rising temperature reflectivity increases from 0.06 at 1200 K to 0.40 at 2000 K for phenol glass reinforced plastic, and from 0.05 at 1200 K to 0.38 at 1900 K for composite with quartz filler. This is so because heating entails the decomposition of the binder in the surface are largely determined by the characteristics of the filler or its melt whose reflectivity is higher than that of the coke residue of phenol resin. For the same reason treatment of a specimen in a plasma ensures higher values of $\rho_{\lambda n}$ which change less substantially with rising temperature (curves 2, Fig. 1a, b). A characteristic feature of material based on a composite of carbon or

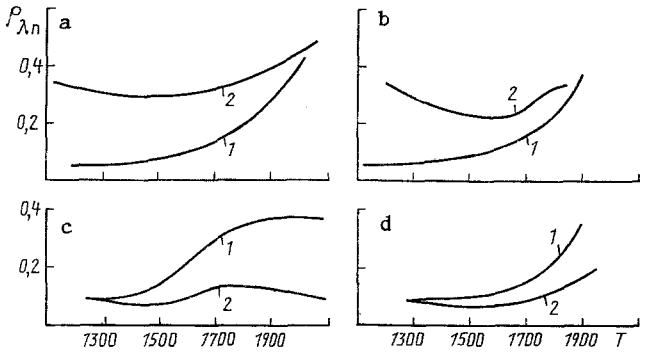

Fig. 1. Normaly hemispherical reflectivity of phenol plastics on the wavelength 0.58 μm: a) composite based on glass fabric and phenol formaldehyde resin: [1) before treatment, 2) after treatment in plasma flux; b) composite based on quartz fabric and phenol formaldehyde resin [1) before treatment, 2) after treatment]; c, d) $\rho_{\lambda n}$ of the structural components of composite based on quartz fabric and phenol formaldehyde resin before and after treatment in a plasma flux, respectively [1) "insertion," 2) carbon fabric]. T, K.

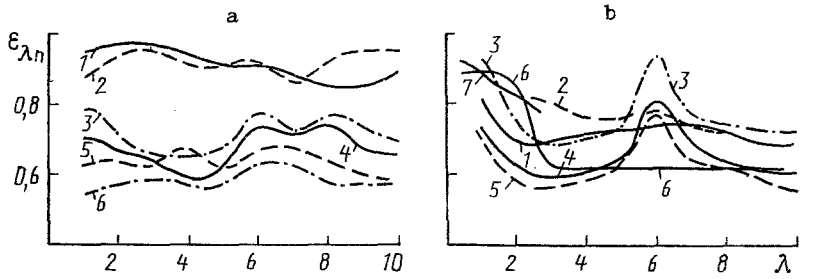

Fig. 2. Radiant emittance of composite based on carbon and quartz fabric and phenol formaldehyde resin: a) before treatment in plasma flux (1), 1310 K; 2, 1430; 3, 1550; 4, 1660; 5, 1800; 6) 1980 K); b) after treatment (1, 1250 K; 2, 1330; 3, 1570; 4, 1670; 5, 1800 K; 6, phenolic graphite, T = 2500 K [5]; 7, phenolic carbon, T = 2550 K [3, 4]), λ, μm.

quartz fabric and phenol formaldehyde resin is the substantial difference between the optical properties of the structural components: the carbon fabric and the threads of the quartz-base insertion. If the $\rho_{\lambda n}$ of the insertion changes with the temperature as substantially as the $\rho_{\lambda n}$ of phenol glass reinforced plastics, then the reflectivity of the carbon base depends much more weakly on the temperature (see curves 2, Fig. 1c, d).

Information on the radiative properties of CM in the spectral range 0.6-10 μm is of considerable interest. Firstly, in this range the predominant part of the proper thermal radiation of the coating is concentrated. The values of $\varepsilon_{\lambda n}$ obtained in this range therefore make it possible to calculate the proper radiation of the material which in some cases plays a substantial role in the balance of thermal fluxes. The value of the optical characteristics in the mentioned range is also indispensable for the calculation of radiative and convective heat exchange in high-temperature plant.

Spectral normal radiant emittance is measured by comparing the radiation of a specimen of the investigated material and of the model of a blackbody with the same temperature by the relation

$$\varepsilon_{\lambda n} = \frac{I^{\circ}_{\lambda n}}{I^{\mathrm{bl}}_{\lambda n}}, \quad (2)$$

where $I^{0}_{\lambda n}$, $I^{\mathrm{blb}}_{\lambda n}$ is, respectively, the spectral normal brightness of the specimen and of the

blackbody. To determine the true temperature of the sighted surface of the specimen we used the values of $\varepsilon_{\lambda n}$ on the wavelength 0.58 μm calculated in accordance with Kirchhoff's law on the basis of the data for $\rho_{\lambda n}$. The model of the blackbody was made in the form of a graphite tube heated by electric current, with a rectangular slit in the lateral surface. A description of the installation and of the method of measurements is provided in [9].

The results of measurement of $\varepsilon_{\lambda n}$ of CM based on carbon and quartz fabrics and phenol formaldehyde resin are presented in Fig. 2. It can be seen that $\varepsilon_{\lambda n}$ changes slightly with a change of wavelength, and that it depends strongly on the temperature. With rising temperature radiant emittance decreases, changing within very broad limits: from 0.97 with λ = 2.5 μm, T = 1310 K to 0.55 with λ = 1 μm, T = 1980 K. After a plasma flux has acted, this heat-protective composite shows a fairly strong dependence of $\varepsilon_{\lambda n}$ on λ whose characteristic feature is that at T > 1500 K a maximum appears in the region of 6 μm. Its existence is due to the influence of silicon oxide contained in the investigated material. The data on $\varepsilon_{\lambda n}$ of the coke residue of phenolic graphite at T = 2500 K presented in the same figure and obtained in [5] testify in favor of this assumption since the shape of the dependence $\varepsilon_{\lambda n}(\lambda)$ is analogous to the obtained curves, except for the section of λ = 5-7 μm (the zone of the maximum). For the sake of comparison the results of measurements of $\varepsilon_{\lambda n}$ of the coke residue of phenolic carbon at T = 2550 K in the spectral region 0.4-2.8 μm, obtained in [3, 4], are also given. It can be seen that in all cases there is a tendency of $\varepsilon_{\lambda n}$ to decrease with increasing wavelength in the spectral region 0.6-3 μm.

Figure 3 presents the results of measurement of $\varepsilon_{\lambda n}$ of a composite based on glass fabric and phenol formaldehyde resin. A characteristic feature of material not subjected to treatment in a plama jet is the substantial increase of $\varepsilon_{\lambda n}$ at T = 1600 and 1830 K when the wavelength changes from 1 to 6 μm. Radiant emittance also changes substantially with rising temperature. For instance, on the wavelength 1 μm $\varepsilon_{\lambda n}$ decreases from 0.92 at T = 1300 K to 0.60 at T = 1830 K. After treatment in a gas–plasma jet the dependence $\varepsilon_{\lambda n}(\lambda)$ is characterized by having a maximum of $\varepsilon_{\lambda n}$ in the region of 6-7 μm. The change of $\varepsilon_{\lambda n}$ with rising temperature is less pronounced. For instance, with λ = 1 $\varepsilon_{\lambda n}$ varies from 0.82 at T = 1470 K to 0.66 at T = 1780 K.

Figure 4a, b presents data on the properties of composite of quartz fabric and phenol formaldehyde resin. With specimens not subjected to a plasma jet $\varepsilon_{\lambda n}$ increases with the wavelength increasing in the range 1-7 μm. For instance, at T = 1910 K $\varepsilon_{\lambda n}$ changes from 0.58 for λ = 1 μm to 0.80 for λ = 7 μm. Analogous behavior in the range 2-7 μm is also found in specimens after treatment in gas–plasma flux. With rising temperature the values of $\varepsilon_{\lambda n}$ in the range 1-4 μm increase.

The strong dependence of $\varepsilon_{\lambda n}$ on λ in the investigated materials, as well as a number of special features in their behavior can be explained in the following manner. At high temperatures the principal components of the composites under study are carbon (coke residues of phenol formaldehyde resin, carbon fabric) and silicon dioxide, the principal component of glass and quartz fabric. Their radiant emittance is unequal. For instance, coke residues of phenol formaldehyde resin have a high degree of blackness in the region up to 1 μm, in the range 1-3 μm their radiant emittance decreases. Silicon dioxide is characterized by low radiant emittance in the region up to 1-2 μm and its abrupt increase in the spectral range 2-5 μm. Depending on which of the components predominates in the surface layer, the optical properties change, too, and the characteristics of the predominating component also dominate. Thus, especially the influence of the properties of silicon dioxide explains the increase of $\varepsilon_{\lambda n}$ in the region 2-6 μm in Figs. 2a (curves 3, 4) and 3. As a result of interaction of opposing tendencies in the change of $\varepsilon_{\lambda n}$ of the structural compon-

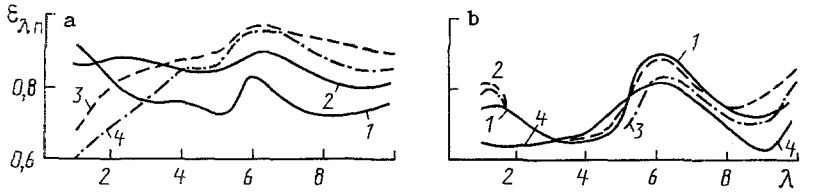

Fig. 3. Radiant emittance of composite based on glass fabric and phenol formaldehyde resin: a) before treatment in plasma flux [1) 1300 K, 2) 1400, 3) 1600, 4) 1830 K)]; b) after treatment [1) 1200 K, 2) 1470, 3) 1560, 4) 1780 K)].

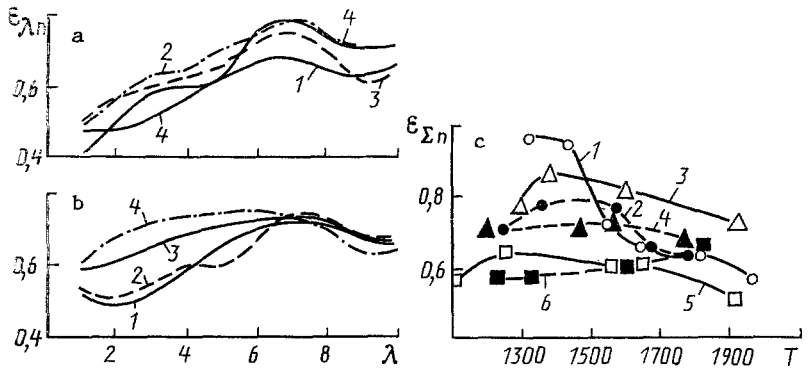

Fig. 4. Radiant emittance of phenolic plastics: a) composite based on quartz fabric and phenol formaldehyde resin before treatment in plasma flux [1) 1180 K, 2) 1260, 3) 1560, 4) 1910 K]; b) the same, after treatment [1) 1230 K, 2) 1320, 3) 1600, 4) 1830 K]; c) phenolic plastics with filler [1) carbon and quartz fabric before treatment in plasma flux; 2) the same, after treatment; 3) glass fabric before treatment; 4) the same, after treatment; 5) quartz fabric before treatment; 6) the same, after treatment].

ents, an increase of the wavelength (decrease for coke and increase for silicon dioxide) entails the appearance of characteristic features in the spectral curves $\varepsilon_{\lambda n}(\lambda)$ of the composite: a minimum of $\varepsilon_{\lambda n}$ in the section 2-4 μm (see Figs. 2b, 3b, 4b), a maximum in the range 5-7 μm (see Figs. 2b, 3b).

The decrease of the values of $\varepsilon_{\Sigma n}$ with rising temperature for phenolic plastic based on carbon and quartz fabric (see Fig. 4c, curve 1) can be explained analogously, i.e., by the increased influence of the optical properties of quartz on the radiant characteristics of the composite upon partial burn-out of carbon and the destruction of phenol formaldehyde resin in the surface layer. The integral normal degree of blackness of that same material after treatment in a plasma flux changes less substantially because this process occurred partly at the stage of plasma treatment.

It is also clear from Fig. 4c that in all cases, both before and after treatment in the plasma jet, the values of $\varepsilon_{\Sigma n}$ for materials with filler of glass fiber are higher than for composite with quartz fabric, although the content of binder in the latter case is even somewhat higher (by 6%). This may be due to the circumstance that on account of the lower heat resistance of glass fabric the percent content of carbon in the surface layer of the speciment proves to be larger than in material with quartz fabric. It should be noted that $\varepsilon_{\Sigma n}$ is essentially the partial integral radiant emittance. Its values were calculated from the results of measurements of $\varepsilon_{\lambda n}$ in the range 1-10 μm and with the use of data on $\varepsilon_{\lambda n}$ on the wavelength 0.58 μm and the approximation of the values of $\varepsilon_{\lambda n}$ to the spectral region 0.58-1 μm. In the mentioned spectral range 0.58-10 μm for the temperature range under study from 94% (at T = 1200 K) to 97% (at T = 2000 K) of the blackbody radiation is concentrated (on the section of approximation 0.58-1 μm from 0.02% (at T = 1200 K) to 6% (at T = 2000 K), which testifies to the closeness of the calculated values of $\varepsilon_{\Sigma n}$ to the values of the full integral normal degree of blackness.

It has to be pointed out that in the experiments heating of the investigated materials proceeded fairly slowly with successive transition from lower to higher temperatures. The specimens were also held for a long time at the temperatures at which measurements were carried out so that coking and other possible physicochemical changes would proceed fully in the investigated part of the surface of the specimen.

It follows from the data presented above that on the whole there is a great variety in the properties of the investigated materials and their change in dependence on the wavelength, the temperature, the effect of plasma fluxes, that is due to the difference between the optical characteristics of the structural component of the composite concerned.

NOTATION

q, heat flux; τ, time of action; λ, wavelength; T, absolute temperature; $\rho_{\lambda n}$, normally hemispherical reflectivity; $\varepsilon_{\lambda n}$, spectral normal radiant emittance; $\varepsilon_{\Sigma n}$, partial integral normal radiant emittance; $I_{\lambda n}$, spectral normal brightness; λ_i, emission line of mercury vapors; $\lambda_j = 0.60$ μm. Superscripts: s, summary proper and reflected radiation; o, specimen; st, standard; blb, blackbody.

LITERATURE CITED

1. Sh. Park, Dzh. Kh. Landell, M. Dzh. Grin et al., Aérokosm. Tekh., 3, No. 5, 50-61 (1985).
2. N. A. Rubtsov and E. I. Averkov, Promyshlen. Teplotekh., 5, No. 5, 75-87 (1983).
3. R. G. Uilson and K. R. Spitser, Raket. Tekh. Kosmon., 6, No. 4, 108-117 (1968).
4. R. G. Uilson and K. R. Spitser, Raket. Tekh. Kosmon., 7, No. 11, 117-119 (1969).
5. Dzh. Kh. Cheng and G. V. Satton, Raket. Tekh. Kosmon., 7, No. 6, 147-153 (1969).
6. R. B. Poup, Raket. Tekh. Kosmon., 3, No. 12, 235-237 (1967).
7. L. S. Slobodkin, M. Ya. Flyaks, and B. V. Andreev, Inzh.-Fiz. Ah., 42, No. 3, 442-448 (1982).
8. L. S. Slobodkin and M. Ya. Flyaks, Heat and Mass Exchange: Achievements and Prospects, [in Russian], Minsk (1985), pp. 115-118.
9. L. S. Slobodkin and M. Ya. Flyaks, Heat and Mass Exchange: Physical Fundamentals and Research Methods [in Russian], Minsk (1980), pp. 106-108.

PHASE TRANSITION KINETICS IN IRON AND STEEL DURING HEATING

S. I. Mednikov and D. M. Gureev

UDC 621.373.821.038.823:621.78

Similarity theory is used to analyze phase transformations in iron and steel during heating. A kinetic equation is obtained by assumption of self-similarity of the phase transition. Experimental data are processed and effective kinetic parameters determined. It is concluded from the results obtained that the elementary act of phase transition consists of a cooperate transition into the new phase of regions containing $(1\text{-}2)\cdot 10^2$ atoms.

I. A large number of studies [1-4] have been dedicated to the kinetics of phase transitions in iron and steel. Theoretical studies of hardening have been directed mainly toward a search for some single micromechanism controlling phase transitions, for example, carbon diffusion [1, 5]. However critical analysis of the results of [2, 6-8] does not permit the conclusion that such an approach is universal.

The complexity of theoretical description of phase transition kinetics is the result of simultaneous occurrence of a number of subprocesses (lattice readjustment, dopant redistribution, formation, movement, and annihilation of defects, etc.), among which it is difficult to establish valid quantitative cause–effect relationships. Therefore it is of interest to use the methods of similarity theory to analyze phase transition kinetics. In fact, analysis shows that simplification of the process is possible only in the case of self-similar occurrence of the phase transition, i.e., in the case of similarity of all subprocesses [3, 9, 10]. In [9] the criterion for quasistatic occurrence of the process was introduced

$$Q = \exp(-\Delta G/RT), \quad (1)$$

where ΔG is the motive force and T is temperature. Here $Q \simeq 1$ corresponds to thermodynamic equilibrium, and $Q \simeq 0$ to self-similar behavior. As was shown in [9], at $Q \simeq 0$ all internal

Samara Branch, P. N. Lebedev Physics Institute, Academy of Sciences of the USSR.

Translated from Inzhenerno-fizicheskii Zhurnal, Vol. 61, No. 4, pp. 669-672, October, 1991. Original article submitted September 9, 1990.

0022-0841/91/6104-1293$12.50